Influence of morphology on the transport properties of polystyrene/polybutadiene blends: 2. Modelling results

N. Shah, J. E. Sax and J. M. Ottino
Departments of Chemical Engineering and Polymer Science and Engineering, University of Massachusetts, Amherst, MA 01003, USA
(Received 28 September 1984; revised 21 January 1985)

Unsteady-state and steady-state models are used to predict the effective diffusion coefficients, D_{eff}, of small molecules in randomly interspersed polystyrene–polybutadiene blends and comparisons are made with experimental values obtained by sorption measurements. It is found that the polybutadiene and polystyrene phases are not topologically equivalent. This fact is responsible for the discrepancies between the experimental values of D_{eff} and the predictions from standard steady-state models.

Simulations of sorption experiments based on an unsteady-state model have shown that values of D_{eff} obtained by different methods from the same sorption experiment differ consistently from each other. This supports the hypothesis that the experimentally observed differences between the various values of D_{eff}, for a given blend–permeant pair, can be justified solely on the basis of morphological arguments.

(Keywords: morphology; transport; disordered media; models; polymer blends)

INTRODUCTION

A large fraction of polymer blends have morphologies that can best be described as chaotic, i.e., they can be specified in a statistical sense. This is true for many blends prepared by melt mixing of homopolymers. In many instances, one is interested in the transport of gases in these materials. Applications arise in a variety of areas: transport in packaging films, photographic materials, etc. However, the number of suitable predictive models is small and there are few explicit comparisons with experimental data.

Experimentally, the effective diffusion coefficient, D_{eff} (cm^2/s) is determined on the basis of transient experiments, such as sorption and differential permeation. Usually, one of several techniques is used to compute (and define) D_{eff} from the transient data. For example, when sorption data are available, estimates of D_{eff} can be made by the Initial slope, Halt-time and Limiting-slope methods[1]. As these estimates provide identical values for single-phase materials, they have been assumed in the literature to be equivalent for binary composites also. However it seems likely that some morphological insight may be derived from an in-depth comparative study of the estimates of D_{eff} obtained by the various methods for a given blend.

It is obvious that there is a pressing need for models capable of simulating transient experiments. Although there are models for transient transport processes in composite media in the literature[2], they have not been used to mimic either sorption or permeation. Ottino and Shah[3] reviewed some of these descriptions and presented some preliminary simulations of transient sorption and permeation processes in composites in which both phases had equal solubilities.

This article is concerned with the predictions of D_{eff} for randomly interspersed polymer blends with the help of steady-state and unsteady-state models. Emphasis is placed on morphological effects rather than on anomalous transport in the polymer phases. The model predictions are compared with the experimental data from Sax and Ottino[4], hereafter referred to as (I). Probably, one of the most significant results obtained in (I) is that the different methods used to obtain D_{eff} from sorption data are not equivalent. Different estimation techniques provide different, reproducible values of D_{eff} for the same penetrant–blend pair. These results cannot be explained in terms of any existing model. In this work, we will attempt to explain these differences, establish the limitations of the sorption experiment, and discuss its use in probing the morphology of a given blend.

MORPHOLOGICAL INFORMATION

A superficial examination of the micrographs studied in (I) seems to indicate that the two phases are chaotically interspersed. However, an in-depth examination reveals differences in the characteristic geometry of the clusters of the two phases. On one hand, polybutadiene (PB) tends to form ramified clusters, that is, clusters with a high surface-to-volume ratio. On the other hand, polystyrene (PS) tends to form predominantly compact clusters, that is, clusters with a low surface-to-volume ratio. Let ϕ_B denote the volume fraction of PB in these blends. Due to its geometry, the PB phase tends to form sample-spanning clusters at a fairly low volume fraction, ϕ_B^c. For the same reason, PS becomes disconnected also at a fairly low value of ϕ_B. Above this volume fraction, ϕ_A^c, the PS phase is no longer continuous.

It is necessary to try to identify the volume fractions at which these transitions occur. The locations of these two points have a significant effect on the transport and mechanical properties of the blends under consideration. The relevant transport property for these blends is the

0032-3861/85/081239-08$03.00

effective permeability, P_{eff} (defined by the product of the effective diffusion coefficient, D_{eff}, and the effective solubility, S_{eff}) because the phases differ in their solubilities[2]. The relevant mechanical property is the effective tensile modulus.

The transport data in (I) can be used to determine ϕ_B^c because the value of P_{eff} undergoes its sharpest change at this volume fraction. It is known that, at ϕ_B^c, the effective permeability of the blend is given by[5]:

$$P_{eff} = K P_A^{1-u} P_B^{u} \quad (1)$$

where P_A and P_B are the permeabilities of the PS and PB phases respectively, and $u = t/(t+s)$. It is believed that in three dimensions, $t = 1.95$[6], $s = 0.7$[7] and $K = 0.96$[8].

The value of P_{eff} is calculated for each blend–permeant pair from the product of D_{eff} (from the half-time method) and S_{eff} defined, with little error, by a volume fraction average of S_A and S_B, the solubilities of the PS and PB phases respectively (neglecting any synergistic effects). The experimental value of S_{eff} is not used due to its high degree of uncertainty. The value of P_{eff} at ϕ_B^c is computed for each permeant, from the above equation. Then, ϕ_B^c is calculated by interpolation between the known values of P_{eff}. The value of ϕ_B^c, based on all three permeants, is 0.18 ± 0.04.

The value of ϕ_A^c can be estimated from the ϕ_B dependence of the effective tensile moduli of the blends. The largest change in the effective moduli occurs at ϕ_A^c, above which the PS phase is completely discrete (*Figure 1*)[9]. It can be shown that, at ϕ_A^c, there is an inflection point in the plot of effective moduli *versus* volume fraction[9]. The inflection in this system of blends is found to be at 0.58.

It is noteworthy that $\phi_A^c \neq 1 - \phi_B^c$. This is a clear indication that the two phases are *not topologically equivalent*. This conclusion is supported by the skewed nature of the plot of intermaterial area density *versus* ϕ_B shown in (I). Thus, the morphology of a blend with a volume fraction ϕ_B is not identical to that of a blend with a volume fraction $1 - \phi_B$.

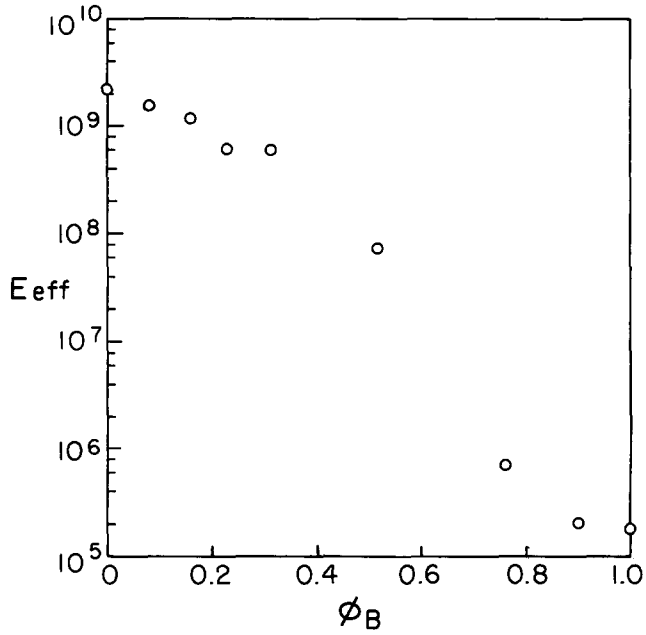

Figure 1 Effective tensile modulus, E_{eff} (N/m^2), of PS/PB blends *versus* volume fraction of PB, ϕ_B. The standard deviation of these data is 6%

STEADY STATE

Theory

Although the phases in these blends are not topologically equivalent, the morphology is still chaotic as there are no apparent signs of order at any scale. Therefore, it is natural to use theories based on this assumption for the prediction of D_{eff}. Two steady-state theories are especially useful for this purpose: Effective Medium Theory (EMT) and Real-Space Renormalization Group Theory (RSRG). In both these theories, the two phases are assumed to be topologically equivalent and the morphology is assumed to be perfectly chaotic.

EMT involves the replacement of the real binary composite by an 'effective' medium whose transport coefficient is computed by averaging over the heterogeneities in the real composite. This is a lattice-based theory and corresponds to a bond-percolation model on the lattice selected to represent the composite. Ideally, EMT is valid only when the scale of heterogeneities is small enough so that there is no 'overlap' between the disturbances caused in the overall potential field by these heterogeneities. Hence, its validity is questionable in the critical region around the percolation threshold of the lattice being used to model the composite, as the length scale of the heterogeneities is then on the order of the size of the sample. However, it provides accurate predictions of D_{eff} at other compositions, as long as the morphology is chaotic.

EMT was originally developed for composites whose phases have identical solubilities[10]. Davis[11] made suitable modifications to extend its applicability to composites whose phases differ in their solubilities. An identical result is obtained if the conductivities in the original EMT equation[10] are replaced by permeabilities and S_{eff} is defined, as before, by the volume fraction average. D_{eff} for such composites is given by:

$$D_{eff} = \frac{D_B}{S\left\{1 + \phi_B \dfrac{(1-S)}{S}\right\}}\left[A + \left(A^2 + \frac{2}{(z-2)} Sx\right)^{1/2}\right] \quad (2)$$

where $A = \dfrac{(z/2)\phi_B - 1 + Sx\{(z/2)(1-\phi_B) - 1\}}{z-2}$

$S = S_A/S_B$; $x = D_A/D_B$; z = coordination number

An analysis of transport in terms of this model has been presented by Sax and Ottino[12].

RSRG is an analytical technique which gives estimates of the effective transport coefficients of composites over the entire composition range, including the critical region. A review of the various forms of RSRG and its applications has been provided by Burkhardt and van Leeuwen[13]. Several investigators have used RSRG to evaluate the effective conductivities of dilute resistor networks (networks containing conductors and insulators), especially around the percolation threshold of the network[14–16]. Recently, Shah and Ottino[17] extended the method to evaluate the effective transport coefficients of random, space-filling, two- and three-phase composites in two and three dimensions. The reader is referred to that work for details of the technique.

The essence of the method lies in the representation of the composite by a regular tessellation, whose individual cells represent either one phase or the other (site-percolation model). Instead of the individual cell, a representative group of cells can be considered to be the primary building block of the tessellation. Such a group, called a renormalization cluster, may contain any conceivable configuration of phases and hence could be homogeneous or heterogeneous depending on whether it contains one phase or both.

The aim of the renormalization process is to replace the original heterogeneous tessellation by an equivalent homogeneous tessellation whose effective transport coefficient is known. This is achieved by a sequence of averaging operations at the scale of the renormalization cluster. For this purpose, it is necessary to classify every configuration of phases in the renormalization cluster according to the effective transport coefficient of the cluster with that configuration.

At every step of the process, a new tessellation is created by replacing every renormalization cluster in the old tessellation by a single cell, whose transport coefficient is equivalent to the effective transport coefficient of the particular cluster. Although this results in the creation of a multi-phase tessellation, it is approximated by a tessellation containing two pseudo-phases, each of whose transport coefficient is a weighted average of those of the phases assimilated into the pseudo-phase. The morphology is assumed to remain random at each step and the volume fraction of the pseudo-phase with the higher transport coefficient in the new tessellation is related to that in the old tessellation through the renormalization group transformation.

This process is repeated until the group transformation reaches one of its stable fixed points. At this point, the tessellation contains only one pseudo-phase and is practically homogeneous. The effective transport coefficient of the original composite is then given by that of the tessellation at the fixed point, which in turn is equal to that of the only remaining pseudo-phase.

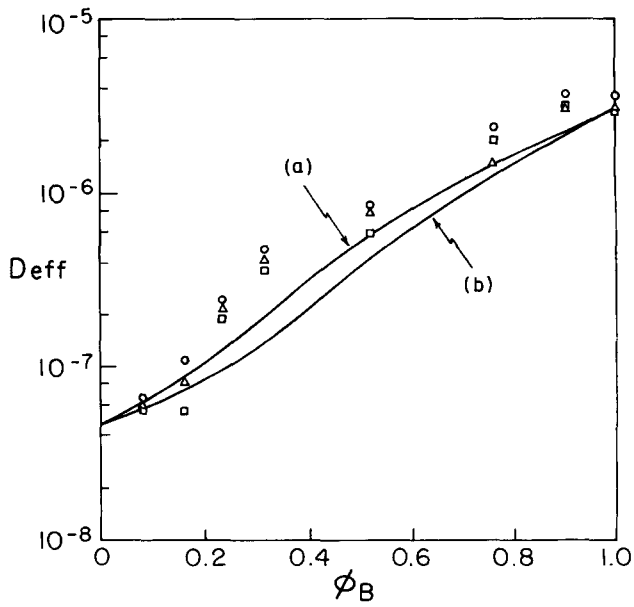

Figure 2 Comparison of effective diffusion coefficients determined by initial-slope method (○), half-time method (△), and limiting-slope method (□), with predictions from (a) EMT and (b) RSRG. Data correspond to diffusion of CO_2 in PS/PB blends at 25°C

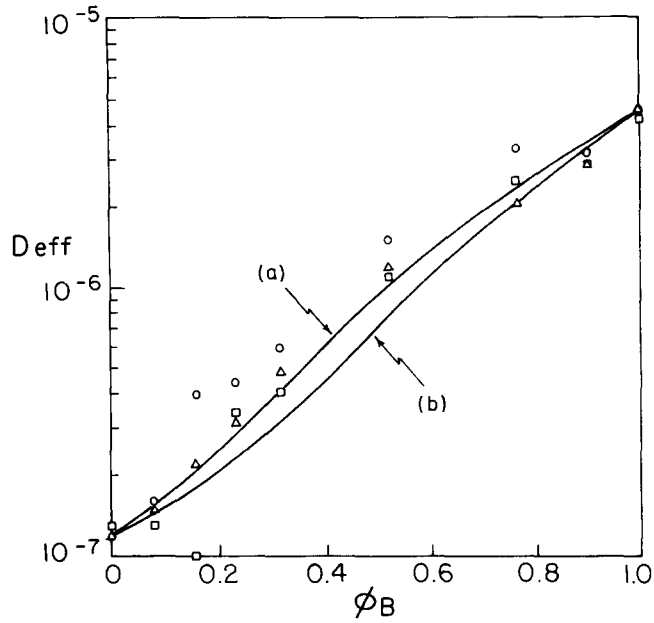

Figure 3 Comparison of effective diffusion coefficients determined by initial-slope method (○), half-time method (△) and limiting-slope method (□), with predictions from (a) EMT and (b) RSRG. Data correspond to diffusion of O_2 in PS/PB blends at 25°C

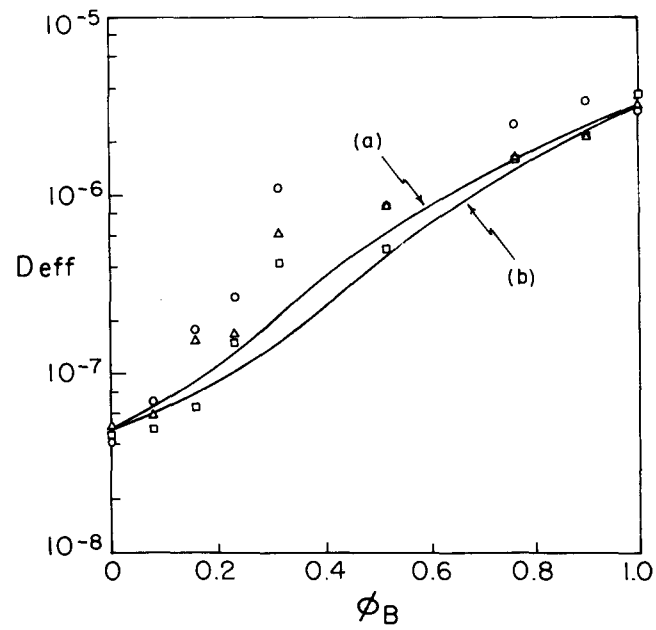

Figure 4 Comparison of effective diffusion coefficients determined by initial-slope method (○), half-time method (△) and limiting-slope method (□), with predictions from (a) EMT and (b) RSRG. Data correspond to diffusion of N_2 in PS/PB blends at 25°C

Results and analysis

Figures 2, 3 and *4* show the comparison between the experimental data from (I) and the predictions from EMT and RSRG. The three-dimensional cubic lattice is used for both theories. One fact stands out immediately: Both theories tend to underestimate the value of D_{eff}, especially in the range $0.2 < \phi_B < 0.5$.

The EMT and RSRG models are inadequate for the PS/PB system because the phases in these blends are not topologically equivalent. The major consequence of this fact is that ϕ_B^c is quite low (~ 0.2). This is much lower than

that obtained from either model (~ 0.3). This explains why the data for blends in the range $0.2 < \phi_B < 0.3$ are so drastically underestimated. Although, in this range, the blends are actually bicontinuous, the PB phase is still considered discrete in both models because the volume fraction is still below the percolation threshold.

At higher volume fractions, the predictions come much closer to the experimental data. In this range, the experimental values of D_{eff} are higher than expected because PS becomes discontinuous at a lower value of ϕ_B than that for the cubic lattice used in both theories. However, here the discrepancies are less pronounced because the change in D_{eff} due to the breakdown of the last continuous cluster of PS is much smaller than that caused by the formation of the first continuous cluster of PB.

This analysis of the discrepancies between predictions and data does not consider any special morphological features that may have been built in during the sample preparation process and may not be visible in the micrographs. The tendency of PB to form ramified clusters is due to its low viscosity compared to that of PS during the blend formation process. The high mobility of PB might allow it to move close to the boundary of the film during its moulding stage. The resultant increase in accessibility of PB clusters from the boundary would enhance the underestimation of the data by the two theories.

UNSTEADY STATE

Theory

The transient process of sorption of a permeant can be simulated by representing the composite by a regular tessellation created by dividing space into identical, regular, convex domains, or cells, each of which is in contact with the same number of neighbours. In two dimensions, tessellations may be built with triangular, square or hexagonal cells and in three dimensions, they may be composed of cubic cells.

The simulations in this article are based on a two-dimensional hexagonal tessellation. A two-dimensional tessellation was chosen so as to minimize the expense of carrying out simulations and the hexagonal geometry was selected because its co-ordination number is the highest among regular two-dimensional tessellations and is equal to that of the two-dimensional Voronoi tessellation (which has a random topology and geometry). The two-phase nature of the blend is simulated by labelling the cells either A or B. The morphology being modelled dictates the number and locations of the two types of cells. If the morphology is perfectly chaotic, then it is completely specified by the volume fraction, ϕ_B. The probability that a given cell is labelled B is equal to ϕ_B.

The concentration field of any permeant in a blend is obtained by solving the equations for the conservation of mass in all the N cells in the tessellation representing the blend. (The mass conservation equation for each cell is often referred to as the master equation[18], which is the precursor of the Fokker–Planck and the diffusion equations.) The average concentration, C_i, in any cell i with j nearest neighbours is given by:

$$dC_i/dt = \sum_j W_{ij}(K_{ij} - C_i) \tag{3}$$

The concentration field is obtained by solving this set of coupled, linear, ordinary differential equations with the appropriate boundary conditions. Sorption boundary conditions are imposed in the flux direction and cyclic boundary conditions are imposed in the direction normal to the flux. Physically, these boundary conditions simulate sorption into a semi-infinite film with a finite thickness. Here, W_{ij} is a transition rate for diffusion of the permeant between cells i and j. Ottino and Shah[3] have related W_{ij} to the diffusion coefficients of the two phases and the parameters that define the geometry of the cells constituting the tessellation. K_{ij} is the ratio of the solubility of the permeant in the phase represented by cell i to that in the phase represented by cell j. When cells i and j represent the same phase, W_{ij} is directly proportional to the diffusion coefficient of that phase. When they represent different phases, W_{ij} is assumed to be proportional to the diffusion coefficient of the less permeable phase. The last assumption results in conservative estimates of D_{eff}. (It is clear that if $N \to \infty$ and $\{W_{ij}\}$ are selected 'appropriately', this model would provide 'exact' solutions to transport problems in composites with any arbitrary morphology.)

The dimensionless variables are defined as follows:

$$\bar{C}_i = C_i/C_b$$

where C_b is the gas phase concentration of the permeant,

$$\tau = W^0 t$$

where τ is the dimensionless time and W^0 is the transition rate between cells containing the more permeable phase, and

$$R_{ij} = W_{ij}/W^0$$

where R_{ij} is either unity or equal to the ratio of the diffusion coefficients of the two phases, depending on the identities of i and j.

In dimensionless form, equation (3) can be rewritten as:

$$d\bar{C}_i/d\tau = \sum_j R_{ij}(K_{ij}\bar{C}_j - C_i) \tag{4}$$

For all the interfaces exposed to the gas phase, K_{ij} is equal to the solubility S_i of the permeant in cell i and $\bar{C}_j$ is obviously equal to unity. Assuming Henry's law, this solubility can be defined by:

$$\bar{C}_i = S_i C_g \tag{5}$$

that is, S_i is the ratio of the polymer phase concentration of the permeant to its gas phase concentration, C_g.

The solution of this set of equations provides estimates of $\bar{C}_i$ as a function of τ for all cells i. The mean concentration in the blend is defined by:

$$C_a = \left(\sum_i \bar{C}_i\right)\Big/ N \tag{6}$$

and is proportional to the mass uptake of the permeant in the blend. Neglecting synergistic effects, the equilibrium concentration ($\tau \to \infty$) of the permeant in the blend is given by:

$$C_\infty = [\phi_B S_B + (1-\phi_B) S_A] C_g \quad (7)$$

and is proportional to the equilibrium mass uptake in the blend. Then, the fractional mass uptake (ratio of the mass uptake at time τ to the equilibrium uptake) is given by:

$$M_\tau / M_\infty = C_a / C_\infty \quad (8)$$

Felder and Huvard[1] and Berens[19] provide three methods for evaluating the effective diffusion coefficient, D_{eff}, from sorption measurements.

(a) Initial slope method:

$D_{eff} \sim [\mathrm{d}(M_\tau/M_\infty)/\mathrm{d}\tau^{1/2}]^2$, for $\tau \to 0$
$D_{eff} = D_B[(\text{Initial slope})_{blend}/(\text{Initial slope})_B]^2$

(b) Half-time method:

If $\tau_{1/2}$ is the time at which M_τ/M_∞ becomes equal to 1/2,

$D_{eff} \sim 1/\tau$
$D_{eff} = D_B[(\tau_{1/2})_B/(\tau_{1/2})_{blend}]$

(c) Limiting slope method:

$D_{eff} \sim \mathrm{d}\{\ln(1 - M_\tau/M_\infty)\}/\mathrm{d}\tau$, for $\tau \to \infty$
$D_{eff} = D_B[(\text{Lim. slope})_{blend}/(\text{Lim. slope})_B]$

It should be noted that these three methods are *defining* D_{eff} by analogy with the definitions for a pure material. Of course, for a pure material, all the estimates of D_{eff} should be identical.

Results and analysis

Figures 5, 6 and *7* provide comparisons between the experimental data from (I) and the predictions from the unsteady-state model. Three realizations were carried out for each blend–permeant pair and the mean values have been shown in these Figures. The percentage deviation of the half-width of the 95% confidence interval from the mean value was computed for every method of estimating D_{eff} for each blend–permeant pair. The values range from 1 to 55%. The confidence interval is narrow at low and high values of ϕ_B and is widest, as expected, in the vicinity of the percolation threshold of the tessellation. (Near the percolation threshold, two different realizations may produce two composites with the same volume fraction of PB but with vastly different morphologies: one, in which the PB phase is continuous and the other, in which it is still discontinuous.)

It is noteworthy that the unsteady-state model also provides three different estimates of D_{eff} for each blend–permeant pair. The simulations confirm that the differences between the various estimates of D_{eff} obtained experimentally can be theoretically reproduced without invoking any 'anomalous' behaviour on the part of the blend. The heterogeneity of the blend is at least partly responsible for this phenomenon. This raises the possibility of obtaining some qualitative morphological information from the observed trend in D_{eff} for a given blend.

The simulations underestimate the values of D_{eff} obtained in (I) for several reasons. These are: (1) The site percolation threshold of the two-dimensional hexagonal tessellation is 0.5. Consequently, there is a large difference between the percolation thresholds of the blend system and this tessellation. (2) The simulations were carried out

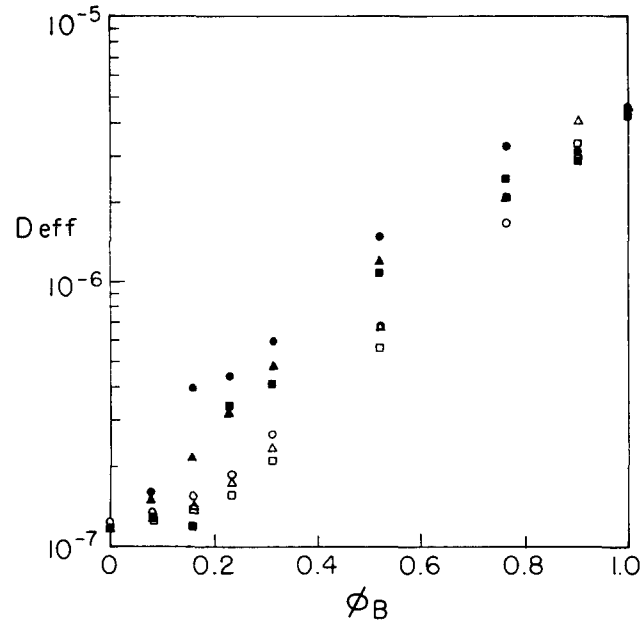

Figure 5 Effective diffusion coefficient, D_{eff}, of O_2 in PS/PB blends *versus* volume fraction of PB, ϕ_B. Filled symbols: experimental data from (I); open symbols: predictions from unsteady-state model

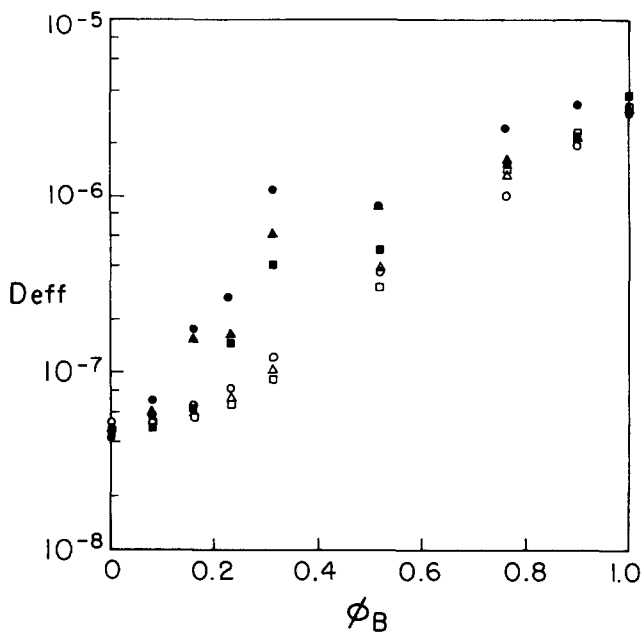

Figure 6 Effective diffusion coefficient, D_{eff}, of N_2 in PS/PB blends *versus* volume fraction of PB, ϕ_B. Filled symbols: experimental data from (I); open symbols: predictions from unsteady-state model

on chaotic composites in which both phases were topologically equivalent. As noted before, the two phases in the blends are not topologically equivalent. (3) A two-dimensional tessellation does not allow bicontinuity and the blends are evidently bicontinuous over a fairly wide range of volume fractions.

The unsteady-state simulations are carried out on the basis of computer-generated composites whose morphology is prescribed by the user. Simulations on a composite with a fixed volume fraction of PB, but with different morphologies, confirm the hypothesis that the relative magnitudes of the various estimates of D_{eff} reflect different aspects of the morphology of the blend. Since it is

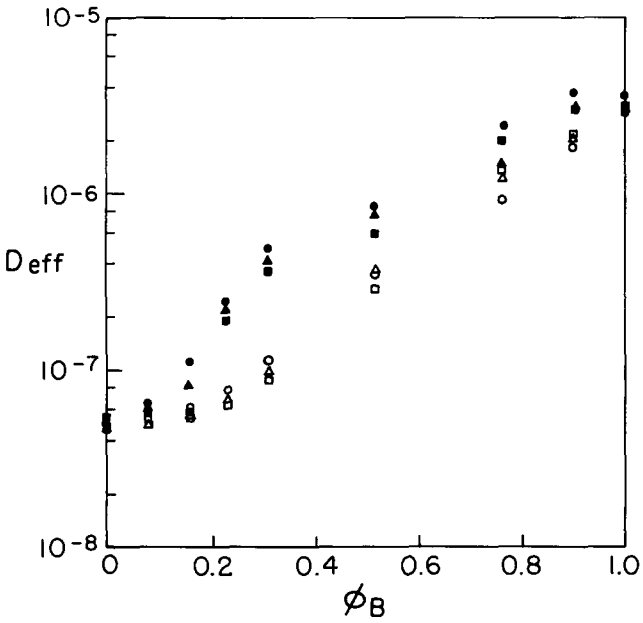

Figure 7 Effective diffusion coefficient, D_{eff}, of CO_2 in PS/PB blends *versus* volume fraction of PB, ϕ_B. Filled symbols: experimental data from (I); open symbols: predictions from unsteady-state model

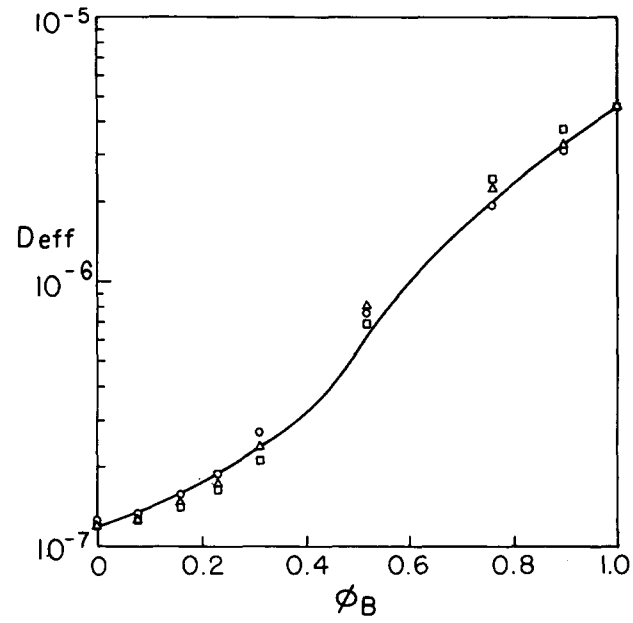

Figure 8 Effective diffusion coefficient, D_{eff}, *versus* volume fraction of PB, ϕ_B. Solid line: RSRG prediction. Data points: unsteady-state model (tessellation size is the same as that used for the results shown in *Figures 5, 6* and *7*)

impossible to duplicate the blend morphology exactly, it is not surprising that the predicted trends in D_{eff} do not correlate exactly with the experimental data.

It may be suspected that the results obtained by the above simulations may be influenced by the finite size of the tessellation. *Figure 8* shows a comparison between estimates of D_{eff} from transient simulations (data points) and those obtained by RSRG (solid line), both based on a two-dimensional hexagonal tessellation. As the RSRG result is thickness-independent, it is clear that the results presented here are not artifacts of the finite size of the tessellation.

MORPHOLOGY DEPENDENCE OF THE TRENDS IN D_{eff}

Since it appears that the various estimates of D_{eff} are affected by different aspects of the blend morphology, it is necessary to understand the factors that influence the D_{eff} trends obtained theoretically and experimentally. It is obvious that all the methods for estimating D_{eff} are dependent on the rate of increase of M_t/M_∞ with time. In the absence of any synergistic effects, M_∞ is a thermodynamic quantity that is fixed for a given blend–permeant pair and can be determined exactly on the basis of the solubilities of the phases and the blend composition. Hence, the rate of increase of M_t is the sole quantity of interest.

M_t is the sum of the mass uptakes in both the phases in the blend. The mass uptake, M_i in phase i, is directly proportional to the average concentration of the permeant in that phase. The rate of increase of the average concentration depends on the diffusion coefficient of that phase, the concentration gradients imposed on the clusters of that phase and the surface area of the clusters. The role of the diffusion coefficient is obvious and as far as surface area is concerned, ramified clusters allow higher rates of mass uptake than compact clusters because of the higher mass flowrates into and through them.

The concentration gradient imposed upon any cluster is dependent on:

(1) Time scale of diffusion of the permeant from the boundary to the cluster (depends on its distance from the boundary and the effective diffusion coefficient of the material separating it from the boundary).

(2) The solubility of the permeant in the cluster. A higher solubility results in a higher concentration gradient.

(3) The average length of the cluster in the direction normal to the boundary at which sorption boundary conditions are imposed. As the rate of decrease of concentration from the boundary of the film to its centre is faster than linear, the concentration gradient on a cluster depends inversely on this average length. Therefore, small clusters have a strong influence on the rate of change of M_i for short times and long clusters exert a milder influence, but for longer times.

The initial slope method is based on the rate of increase of M_i at short times, when the permeant is yet to diffuse significantly into the bulk of the film. The rate is primarily dependent on the composition of the blend on and near the boundary of the film. The accessible area fractions of the two phases determine the ease of entry of the permeant into the film. The surface-to-volume ratio of the clusters in this region also determines the time period for which they exert an influence on the rate.

Usually, the estimate from the half-time method is more representative of the whole composite than either of the other two estimates. By the time M_t/M_∞ is equal to 0.5, the permeant has encountered more of the blend than just the boundary and yet, the experiment is not at the point where almost all the mass uptake is taking place primarily in the matrix phase.

Towards the end of the experiment, the rate of increase of M_i is dictated by the relevant time scales of diffusion into the two phases. These time scales are directly proportional to the square of the average cluster sizes of the phases and inversely proportional to the diffusion

Table 1 Prediction of trends in D_{eff} for blends with specific macroscopic morphological features. Phase A has a lower permeability than phase B. D_{is}, D_{ht} and D_{ls} are estimates of D_{eff} obtained by the initial-slope, half-time and limiting-slope methods respectively

Volume fraction	Morphology			Predictions
$\phi_B \to 0$	Matrix: A. Dispersed B	B is close to the boundary		$D_{is} > D_{ht} > D_{ls}$
		B is randomly distributed		$D_{ht} \sim D_{is} > D_{ls}$
$0 < \phi_B < \phi_B^c$	Matrix: A. Dispersed: B	B is close to the boundary	Compact clusters	$D_{is} > D_{ht} > D_{ls}$
			Ramified clusters	$D_{is} > D_{ht} > D_{ls}$
		B is randomly distributed	Compact clusters	$D_{ht} > D_{is} > D_{ls}$
			Ramified clusters	$D_{ht} > D_{is} > D_{ls}$
$\phi_B^c < \phi_B < 0.5$	Phases are bicontinuous	B clusters are compact		$D_{is} \gtrsim D_{ht} > D_{ls}$
		B clusters are ramified		$D_{is} > D_{ht} > D_{ls}$
$0.5 < \phi_B < \phi_A^c$	Phases are bicontinuous	A clusters are compact		$D_{is} > D_{ht} > D_{ls}$
		A clusters are ramified		$D_{is} > D_{ht} \gtrsim D_{ls}$
$\phi_A^c < \phi_B < 1$	Matrix: B. Dispersed: A	A is close to the boundary	Compact clusters	$D_{ls} > D_{ht} \sim D_{is}$
			Ramified clusters	$D_{is} \sim D_{ls} > D_{ht}$
		A is randomly distributed	Compact clusters	$D_{is} \gtrsim D_{ls} > D_{ht}$
			Ramified clusters	$D_{is} \gtrsim D_{ls} > D_{ht}$
$\phi_B \to 1$	Matrix: B. Dispersed: A	A is close to the boundary		$D_{ls} > D_{ht} \gtrsim D_{is}$
		A is randomly distributed		$D_{is} \gtrsim D_{ls} > D_{ht}$

coefficient. The estimate of D_{eff} from the limiting slope method is more strongly affected by the diffusion coefficient of the phase with the longer time scale. For example, in the PS/PB system, the PS phase has a longer time scale at all volume fractions below ϕ_A^c. But, at higher volume fractions, the PB phase has the longer time scale because the PS phase is only present in the form of small, compact clusters.

Usually, blends prepared by melt-mixing are assumed to have chaotic morphologies. However, as noted before, deviations from this ideal have been found experimentally. One important form of deviation involves the violation of the assumption that a blend is statistically homogeneous. This results in macroscopic spatial deviations from the average value of ϕ_B for the blend (for example, skin–core effects). The other important form of deviation is a consequence of the tendency of one of the phases to form predominantly compact or predominantly ramified clusters. The above observations on the morphology dependence of the various estimates of D_{eff} are useful in qualitatively predicting trends in D_{eff} for blends with morphologies that exhibit such deviations from the ideal of statistical homogeneity (*Table 1*).

These predictions can be checked with the data available in (I) (*Table 2*). For all the bicontinuous blends ($\phi_B = 0.23$, 0.312 and 0.516), there is enough information to predict the trends in D_{eff} correctly. For all the other blends, the micrographs are insufficient for complete characterization and two alternative predictions are available for each blend. In each case, it is found that the experimental trend agrees with at least one of the predictions. This provides additional insight into the morphologies of these blends. It can be concluded that PB is highly accessible from the boundary of the film at all volume fractions, while PS is always randomly distributed in the bulk of the film.

CONCLUSIONS

Several conclusions can be drawn from the above applications of steady-state and unsteady-state theories to the polymer blends described in (I):

(1) Theories based on disordered, lattice-based composites, are inadequate for predicting the behaviour of blends whose components are not topologically equivalent.

Table 2 Comparison of the predicted trends for the blends in (I) with the experimentally observed trends

Volume fraction	Morphology	Prediction	Experimental trends	Conclusions
0.08	Matrix: PS; Dispersed: PB; $\phi_B \to 0$	$D_{is} > D_{ht} > D_{ls}$ or $D_{ht} \sim D_{is} > D_{ls}$	$D_{is} > D_{ht} > D_{ls}$	Clusters of PB are accessible from the boundary
0.1584	Matrix: PS; Dispersed: PB; $0 < \phi_B < \phi_B^c$; clusters of PB are ramified	$D_{is} > D_{ht} > D_{ls}$ or $D_{ht} > D_{is} > D_{ls}$	$D_{is} > D_{ht} > D_{ls}$	Again, PB is freely accessible
0.23 and 0.312	Blends are bicontinuous; $\phi_B^c < \phi_B < 0.5$; clusters of PB are ramified	$D_{is} > D_{ht} > D_{ls}$	$D_{is} > D_{ht} > D_{ls}$	--
0.516	Blend is bicontinuous; $0.5 < \phi_B < \phi_A^c$; clusters of PS are compact	$D_{is} > D_{ht} > D_{ls}$	$D_{is} > D_{ht} > D_{ls}$	--
0.76	Matrix: PB; Dispersed: PS; $\phi_A^c < \phi_B < 1$; clusters of PS are compact	$D_{ls} > D_{ht} \sim D_{is}$ or $D_{is} \gtrsim D_{ls} > D_{ht}$	$D_{is} > D_{ls} > D_{ht}$	PS is randomly distributed in the bulk
0.9	Matrix: PB; Dispersed: PS; $\phi_B \to 1$	$D_{is} > D_{ht} \gtrsim D_{ls}$ or $D_{is} \gtrsim D_{ls} > D_{ht}$	$D_{is} > D_{ht} \sim D_{ls}$	PS is randomly distributed

(2) Sorption and permeation experiments on polymer blends can now be simulated with the help of a new unsteady-state model. Such simulations have also resulted in variations between various estimates of D_{eff} obtained for a given blend–permeant pair. This indicates that the data reported in (I) may be understood on the basis of morphology alone.

(3) The observed trend in D_{eff} is strongly dependent on the morphology of the blend. This is true for both real and computer-generated blends; hence, it is almost impossible to reproduce experimental trends exactly, as the morphology of the actual blend can never be exactly simulated. However, qualitative predictions can be made for the trends in blends with certain types of morphologies if it is assumed that the heterogeneity of the blends is solely responsible for the discrepancies between the various estimates of D_{eff}.

(4) Different effective diffusion coefficients are valid for the same blend depending on the extent of exposure of the blend to the permeant. (The diffusion coefficient appears to be time-dependent.) This fact has important ramifications in the context of the utilization of these blends in permeant-rich environments.

(5) Experimental transport measurements can be used to confirm and complement morphological information obtained from studying micrographs of polymer blends.

ACKNOWLEDGEMENT

This research was supported by the National Science Foundation grant DMR-8020244 and the Center for University of Massachusetts–Industry Research in Polymers.

REFERENCES

1 Felder, R. M. and Huvard, G. S. in 'Methods of Experimental Physics', (Ed. R. A. Fava), **16C**, Academic Press, New York, 1980, p. 342
2 Hughes, B. D. and Prager, S. in 'The Mathematics and Physics of disordered media', (Eds. B. D. Hughes and B. W. Ninham), Lecture Notes in Mathematics, **1035**, Springer-Verlag, New York, 1983, p. 1
3 Ottino, J. M. and Shah, N. *Polym. Eng. Sci.* 1984, **24**, 153
4 Sax, J. E. and Ottino, J. M. *Polymer* 1984, **26**, 1073
5 Straley, J. P. in 'Percolation Structures and Processes', (Eds. G. Deutscher, R. Zallen and J. Adler), Annals of the Israel Physical Society, **5**, The American Institute of Physics, New York, 1983, p. 353
6 Fisch, R. and Harris, A. B. *Phys. Rev. B* 1978, **18**, 416
7 Straley, J. P. *J. Phys. C: Solid St. Phys.* 1976, **9**, 783
8 Solla, S. A. and Ashcroft, N. W. Material Science Center Report No. 5129, Cornell University, 1983
9 Sax, J. E. *PhD Dissertation* 1984
10 Landauer, R. *J. Appl. Phys.* 1952, **23**, 779
11 Davis, H. T. *J. Am. Ceram. Soc.* 1977, **60**, 499
12 Sax, J. E. and Ottino, J. M. *Polym. Eng. Sci.* 1983, **23**, 165
13 Burkhardt, T. W. and van Leeuwen, J. M. J. (Eds.) 'Real-Space Renormalization', Topics in Current Physics, **30**, Springer-Verlag, New York, 1982
14 Bernasconi, J. *Phys. Rev. B* 1978, **18**, 2185
15 Stinchcombe, R. B. and Watson, B. P. *J. Phys. C: Solid St. Phys.* 1976, **9**, 3221
16 Tsallis, C., Coniglio, A. and Redner, S. *J. Phys. C: Solid St. Phys.* 1983, **16**, 4339
17 Shah, N. and Ottino, J. M. *Chem. Eng. Sci.* 1985, in print
18 Reichl, L. E. 'A Modern Course in Statistical Physics', University of Texas Press, Austin, 1980
19 Berens, A. R. *Polymer* 1977, **18**, 697